Power Demand Control Scenarios for Smart Grid Applications with Finite Number of Appliances

John S. Vardakas[a,*], Nizar Zorba[b], Christos V. Verikoukis[c]

[a] *Iquadrat, Barcelona, Spain*
[b] *Qatar University, Doha, Qatar*
[c] *Telecommunications Technological Centre of Catalonia (CTTC), Barcelona, Spain*

Abstract

In this paper we propose novel and more realistic analytical models for the determination of the peak demand under four power demand control scenarios. Each scenario considers a finite number of appliances installed in a residential area, with diverse power demands and different arrival rates of power requests. We develop recursive formulas for the efficient calculation of the peak demand under each scenario, which take into account the finite population of the appliances. Moreover, we associate each scenario with a proper real-time pricing process in order to derive the social welfare. The proposed analysis is validated through simulations. Moreover, the performance evaluation of the proposed formulas reveals that the absence of the assumption of finite number of appliances could lead to serious peak-demand over-estimations.

Keywords: smart grid, demand response, demand scheduling, performance evaluation, analytical model.

*Corresponding author

Email addresses: jvardakas@iquadrat.com (John S. Vardakas), nizarz@qu.edu.qa (Nizar Zorba), cveri@cttc.es (Christos V. Verikoukis)

Nomenclature

$A_{C(j)}$	total average energy cost	$q_{INF}(j)$	distribution of p.u. in use for the *infinite models*
B_m	probability of exceeding P after the acceptance of type-m request	S_m	total number of appliances of type m
$b_{m'}(j)$	control function for FCDS	$s_m(j)$	number of type m active appliances, when the total number of p.u. is j
$b_{m',t}(j)$	control function for FCDS	$SW_{C(j),GC(j)}$	total average social welfare
$C(j)$	cost function	T	number of thresholds for FCDS and FDRS
$c_{m'}(j)$	control function for FDRS	v_m	power-request arrival rate per inactive type-m device
$c_{m',t}(j)$	control function for FDRS	$w_{m,t}$	probability that a consumer will agree to participate in the scheduling program, when $P_{t-1} \leq j < P_t$
$c_{m,t}(j)$	control function for FPRS	*Greek symbols*	
d_m^{-1}	mean appliance operational duration	α_i, β_i	constants that represent the power production cost in generating unit i
$d_{m',t}^{-1}$	mean appliance operational duration when $P_{t-1} \leq j < P_t$	$\gamma_{m'}$	indicator for "elastic"'($\gamma_{m'} = 0$) or "unelastic"($\gamma_{m'} = 1$) appliances
e	predefined upper bound of the blocking probabilities	$\delta_{m',t}$	delay that a type-m' power request suffers under FDRS, when $P_{t-1} \leq j < P_t$
$GC(j)$	total generating cost function	ζ_i	flag that determines if the generating unit i is ON or OFF
j	total number of PU in use	$\eta_i f_i(j)$	no-load cost
M	number of appliances	$\theta_i g_i(j)$	start-up cost
$N_{m'}(j)$	number of type m'-appliances as a function of the number of p.u. in use	$\Lambda_{m',t}$	final power-request arrival rate under FDRS
P	maximum number of supported p.u. in the real system	ξ_i	flag that determines if the generating unit i is shifted from ON to OFF state, or vice versa
p_m	power demand of type-m appliance	*Subscripts*	
$p_{m',t}$	compressed power demand when $P_{t-1} \leq j < P_t$	i	generating unit
P_t	power threshold for the scheduling scenarios	m	appliance type from the M set
Q	distribution normalization constant	m'	appliance type from the $2M$ set
$q_F(j)$	distribution of p.u. in use for the *finite models*	t	power threshold

1. Introduction

The electric power industry confronted numerous challenges in the last two decades. The aging infrastructure, the increasing demands for energy, the limited energy resources, as well as environmental concerns have affected the reliability of the existing power grid [1]. In addition, the rise of new types of loads, such as Electric Vehicles (EVs) will further increase the margin between the installed power capacity and the maximum power output [2]. It is therefore essential to improve the conventional power grid with the aim of increasing the consistency and the efficiency, while providing resilience to equipment failures. The intelligence of the smart grid is the key factor for the provision of improved control, efficiency and safety, through the incorporation of advanced two-way communication capabilities [3].

As the smart grid concept continues to evolve, various methods have been developed in order to support the current infrastructure, such as distributed energy generation, energy storage, smart pricing and demand response (DR) [4], [5]. DR refers to a procedure that is applied in order to motivate changes in the customers' power consumption habits in response to incentives regarding the electricity prices [6]. Various DR algorithms have been presented in the literature that are either based on the scheduling of power requests [7], [8], [9], [10], or on real-time pricing [11], [12], [13], [14], [15], [16]. Under a scheduling scheme, power requests are scheduled to be activated in specific time periods, in order to avoid the overconsumption in high demand hours. For example, in [10] the authors propose a scheme where power demands are delayed in queues, until the total power consumption drops below a predefined threshold. Alternatively, under energy scheduling DR programs [17], power consumption reduction of specific loads is achieved by controlling their operation, in order to consume less power during system stress. The real-time pricing studies focus on the development of tariff models that target on the online participation of the consumers, in order to improve system's performance [18]. As reported in [19], a real-time pricing scheme is most favorable, since it provides a more flattered load curve by reducing the power consumption especially in peak-demand hours.

We have recently proposed four power demand control scenarios that correspond to different approaches on the control of power customers' power demands [20]. All scenarios assume that in each residence a specific number of appliances are installed, with diverse power requirements, different operational times and different power requests arrival rates. The first or the default scenario defines the upper bound of the total power consumption, since it does not consider any scheduling mechanism. The Compressed Demand Scenario (CDS) takes into account the ability of some appliances to compress their power demands and at the same time expand their operational times. Under the Delay Request Scenario (DRS), power requests are delayed in buffers for a specific time period, when the total power consumption exceeds a predefined threshold. A similar threshold is used in the Postponement Request Scenario (PRS), where power requests are postponed not for a specific time period, but until the total power consumption drops below a second threshold. In addition, in [21] we have proposed similar scheduling scenarios and corresponding analytical models that take into account the appliance's feature to alternate between ON and OFF states. The analytical models of both [20] and [21] assume Poisson processes for the power-request arrival procedure, while the models in [21] do not consider the percentage of consumers that refuse to participate in the scheduling program.

In the current paper, we revisit the power demand control scenarios that were presented in [20], and we propose novel and more accurate analytical models for the determination of the peak demand in a residential area. More precisely, in [20] we introduced analytical models for each one of the four power demand control scenarios for the peak-demand calculation, under the assumption of infinite number of appliances in the residential area. This assumption is expressed by a Poisson process for the arrivals of power requests. Nevertheless, when we went to practical implementation of our results within the European project Energy to Smart Grid (E2SG) [22], we noticed an overestimation of the power consumption, so that a change in the developed analytical models must be accomplished, mainly due to our previous assumption in [20] of an infinite number of appliances. Therefore, we leave [20] as an upper bound theoretical study for the four scenarios and here in the current paper we adapt our models to the more realistic assumption of finite number of appliances installed in the area under study. This assumption is expressed by a quasi-random process for the procedure of arrivals of power requests, which is more realistic compared to the Poisson process (infinite number of power-requests' sources).

The main contribution of this paper is the derivation of simple and efficient recursive formulas for the calculation of the peak demand under each scenario, which consider all the aforementioned realistic assumptions. As the simulations later show, the accuracy of the proposed formulas is quite satisfactory. It should be noted that the analytical are obtained by solving the proposed recursive formulas, while the simulation results are obtained from our simulator. The latter is an object oriented simulator, which is based on random numbers for the power-request arrival procedure and executes the rules of each scheduling scenario without using any equations. The comparison of analytical and simulation results also highlights the effectiveness of the proposed analysis, due to the fact that analytical results are obtained in a very short time compared to simulations, which are generally time-consuming and typically performed by troublesome simulation tools. Furthermore, in order to reveal the necessity of the proposed analysis, we compare results from the proposed formulas with corresponding results from [20], which assume infinite number of appliances, and show that the models of [20] results in serious peak-demand overestimations. Finally, we associate each proposed scenario and corresponding analytical model with proper real-time pricing schemes that take into account the specific features of each scenario, in order to derive the social welfare.

The remainder of this paper is organized as follows. In Section II we present the four power demand control scenarios and the corresponding proposed analytical models that tackle a finite number of appliances. In Section III we provide a cost and social welfare analysis, while in Section IV we evaluate the accuracy of the proposed analysis. We conclude the paper in Section V.

2. Finite Power Demand Control Scenarios

2.1. The Default Scenario

We study a residential area, where each residence is connected to the power line through an Energy Consumption Controller (ECC) (Fig. 1). The ECC is connected to all appliances in the residence and it is responsible for the collection and the transmission of power demands of each appliance to the Central Load Controller (CLC). The communication between the ECC of each residence and the CLC is realized through load control messages that are transmitted in the control channel of a Local Area Network (LAN). Under the default scenario, the CLC receives the power demands of all appliances and activates the requests immediately, i.e. no scheduling of requests occurs.

Each residence is equipped with up to M appliances, while the power demand of appliance m ($m = 1, \ldots, M$) is denoted as p_m power units (p.u.). The total number of appliances of type m in the residential area is denoted as S_m. Due to the finite number of each type of appliances, the arrival process of power demands is not random (Poisson arrivals), but it is considered quasi-random, since the total arrival rate of power requests at the CLC is actually a function of the number of inactive appliances. As power requests are generated only from inactive appliances, the total power-request arrival rate is not constant, but it is a function of the variable number of inactive appliances. We denote the arrival rate of power demands per type-m inactive appliances as v_m. The operational time of type-m appliances (the period of a type-m appliance consuming power) is considered to be generally distributed with mean d_m^{-1}. The latter assumption is more realistic compared to the exponential distribution and is applied in several research schemes [20], [21],

[23], since it allows the application of any distribution for the operational times. Furthermore, the maximum number of p.u. that the energy provider can support in the specific area and is denoted as P. In the following analysis, both p_m and P power-consumption parameters are considered discrete, since the developed recursive formulas are based on discrete functions; however, this assumption can provide efficient results, especially when 1 p.u. is considered equivalent to a very small value of the (continuous) power consumption (e.g. 1 $PU \Leftrightarrow 0.01\ W$).

Based on the aforementioned assumptions of the smart grid model, we can determine the distribution $q_F(j)$ that j p.u. are in use in the residential area:

$$jq_F\left(j\right) = \sum_{m=1}^{M} (v_m \cdot d_m^{-1}) p_m q_F\left(j - p_m\right)\left(S_m - s_m(j) + 1\right) \tag{1}$$

for $j = 1, \ldots, P$, and $s_m(j)$ is the number of active appliances of type m in the grid, when the total number of p.u. in use is j. A similar recursive formula is used to determine the distribution of the occupied bandwidth in multi-rate communication networks [24]. In order to calculate $s_m(j)$ we do not follow the complex method used in [24], but we assume that this number can be approximated by the mean number of appliances of type m when an infinite number of appliances is assumed to be present in the grid (Poisson power-request arrivals) and the total number of p.u. in use is j:

$$s_m(j) \approx \frac{(S_m v_m d_m^{-1}) q_{INF}\left(j - p_m\right)}{q_{INF}\left(j\right)} \tag{2}$$

where $q_{INF}(j)$ is the distribution of the number of p.u. in use, when an infinite number of appliances is assumed to be present in the grid. In order to assume equal number of power requests in the two models (infinite and finite cases) the arrival rate in the infinite case is considered to be equal to the product $S_m v_m$, i.e. equal to the arrival rate of requests in the finite case, if all appliances of type m are considered to be inactive. The distribution $q_{INF}(j)$ can be calculated by the following recursive formula [20]:

$$jq_{INF}(j) = \sum_{m=1}^{M} (S_m v_m) d_m^{-1} p_m q_{INF}(j - p_m) \tag{3}$$

where the power-request's arrival rate is equal to the total arrival rate $S_m v_m$ of the case of finite number of appliances. Therefore, in order to derive the distribution $q_F(j)$ of Eq. (1), we first need to solve the recursive formula of Eq. (3), in order to determine the number $s_m(j)$ of the active appliances by using Eq. (2). Both the recursive formulas of Eq. (1) and Eq. (3) can be solved by using an iterative method.

The probability that the total power consumption will exceed P upon the arrival of a power demand for p_m p.u.is given by the summation of the probabilities of all *blocking states*:

$$B_m = \sum_{j=P-p_m+1}^{P} \frac{q_F(j)}{Q} \tag{4}$$

where $Q = \sum_{j=0}^{P} q_F(j)$ is the sum of the un-normalized probabilities $q_F(j)$. Equation (4) can be used to determine the minimum value of the maximum number P of p.u., which guarantees that a power request will not suffer an outage probability not higher than a predefined maximum value e. Therefore, by considering a small value for the threshold e (e.g. 10^{-6}) so that nearly all power requests are accepted, we can use Eq. (1) and Eq. (4) in order to calculate the peak demand.

2.2. The Finite Compressed Demand Scenario

Similarly to the default scenario, the Finite Compressed Demand Scenario (FCDS) considers that the number of appliances in the grid is finite; therefore the arrival process of power requests is quasi-random. The FCDS is applied in cases where there are types of appliances that are able to gradually compress their power demands, and at the same time extend their operational times, e.g. water heaters or air-conditions. The compression of power demands is applied only when the total number of p.u. in use exceeds predefined power thresholds; we consider T thresholds for the p.u. in use. If the total number of p.u. in use is less than the first threshold P_0, then the request is accepted with the initial power demand p_m and operational time d_m^{-1}. In contrast, if the total number of p.u. in use exceeds this threshold, the CLC sends a message to inform all consumers that the power requests of a specific set of appliances will be reduced and at the same time their operational times will be extended, so that the total power consumption is reduced. More specifically, if a consumer wishes to contribute to the peak-demand reduction program, then the power request for a type-m appliance will be accepted with a compressed power demand $p_{m,1} < p_m$, while the operational time of the appliance is extended to a value $d_{m,1}^{-1} > d_m^{-1}$. By considering multiple power thresholds, a gradual reduction of the appliances power demands can be achieved: when the total number of p.u. in use is $P_{t-1} \leq j \leq P_t$ $(t = 1, \ldots, T)$, then consumers are prompted that power-requests for type-m appliances can be accepted with reduced power demand

$p_{m,t}$ and extended operational time $d_{m,t}^{-1}$, with $p_m > p_{m,1} > ... > p_{m,T}$ and $d_m^{-1} < d_{m,1}^{-1} < ... < d_{m,T}^{-1}$. The values of $p_{m,t}$ and $d_{m,t}^{-1}$ for all thresholds should be chosen in such a way so that energy consumption is achieved, i.e. $\left(d_{m,t-1}^{-1} \times p_{m,t-1}\right) > \left(d_{m,t}^{-1} \times p_{m,t}\right)$. An example of the application of FCDS is illustrated in Fig. 2a, where 4 power thresholds are assumed.

It should be noted that the compression of power demands is activated only to "elastic" appliances that have the ability of reducing their power demands and simultaneously extend their operational time, while it is deactivated when the total power consumption drops below the first threshold P_0. To this end, the message that is sent by the CLC to the consumers contains information for the incentives offered to consumers that agree to compress their demands. We consider that a consumer will agree to compress the demand of a type-m appliance, when the current power consumption is $P_{t-1} \leq j < P_t$, with probability $w_{m,t}$, while the consumer will refuse to participate in the program with probability $1 - w_{m,t}$. These probabilities are actually a function of the current power threshold; by considering that the offered incentives are more attractive when the total power consumption is high, more consumers will agree to compress their demands. On the other hand, "un-elastic" appliances that are not able to reduce their power demands (e.g. home entertaining sets of computers) request the same amount of p.u. regardless of the total p.u. in use.

Due to the fact that the probabilities $w_{m,t}$, which denote the consumers' agreement to participate in the demand compression program, affect the power demand arrival rate, two groups for each appliance type should be considered. The first group consists of appliances that are able to compress their demands but they will refuse to participate in the program, while in the second group appliances will agree to contribute to the program by compressing their demands. On the other hand, appliances that are not able to compress their demands could belong to any of the two aforementioned groups. Therefore, in order to derive an analytical model for the peak-demand calculation, $2M$ types of appliances should be assumed; the first M appliances' types comprise the "elastic"appliance population that agree to participate in the program together with half of the "un-elastic"appliances that are unable to compress their demands. The second group consists of the "elastic"appliances population that refuses to participate in the program together with the other half of "un-elastic"appliances. The equal distribution of the "un-elastic"appliances to the two groups is not mandatory; different percentages of the appliance's population in the two groups may be assumed as well. Based on this analysis, the population of appliances $N_{m'}(j)(m' = 1, \ldots, 2M)$ is a function of the number of p.u. in use and is denoted as:

$$N_{m'}(j) = \begin{cases} \frac{S_m}{2} & \text{if } \gamma_{m'} = 0, m' \in 2M, j \in P \\ \frac{S_m}{2} & \text{if } \gamma_{m'} = 1, m' \in 2M, j \leq P_0 \\ S_m w_{m',t} & \text{if } \gamma_{m'} = 1, m' \leq M, (j - p_{m',t}) \in [P_{t-1}, P_t) \\ S_m (1 - w_{m',t}) & \text{if } \gamma_{m'} = 1, m' > M, (j - p_{m',t}) \in [P_{t-1}, P_t) \end{cases} \tag{5}$$

where the parameter $\gamma_{m'}$ is used to express the appliances' ability for demand compression; $\gamma_{m'} = 0$ for "un-elastic"appliances, while $\gamma_{m'} = 1$ for "elastic"appliances. Therefore, since each "un-elastic"($\gamma_{m'} = 0$) appliance type belongs to two groups in the set $[1,\ 2M]$, their population is $S_m/2$ $(m = 1, \ldots, M)$. The same rule applies for "elastic"appliances, when the total number of p.u. in use is less than the first threshold P_0. It should be noted that by considering different percentages for the appliances' population in each group (other than 50% in the first group and 50% in the second group), the two fractions of Eq. (5) should be respectively changed. However, when demand compression is activated, a percentage of the initial S_m appliances will compress their demands (with probability $w_{m',t}$), while the remaining appliances of the same type will continue to operate with their nominal power (with probability $1-w_{m',t}$).

In order to determine a recursive formula for the distribution of the probabilities $q_F(j)$ of the p.u. in use for the set of $2M$ appliances, we define the parameters $p_{m'}$, $p_{m',t}$ and $d^{-1}_{m',t}$, as a function of the values of the parameters of the original set of appliances, so that $p_{m'} = p_{m'+M} = p_m$ for $m' \leq M$, $p_{m',t} = p_{m,t}$ for $m' \leq M$, $p_{m',t} = 0$ for $m' > M$ (since no demand compression occurs for this set of appliances). As far as the operational times are concerned, we define $d^{-1}_{m',t} = d^{-1}_{m,t}$ for $m' \leq M$ and $d^{-1}_{m',t} = 0$ for $m' > M$. Based on these definitions, we proposed the following recursive formula for the determination of the distribution of p.u. in use:

$$
\begin{aligned}
&jq_F(j) = \sum_{m'=1}^{2M} q_F(j-p_{m'})\frac{v_{m'}}{d_{m'}}b_{m'}(j)\left(N_{m'}(j)-s_{m'}(j)+1\right)p_{m'}+\\
&\sum_{m'=1}^{2M}\sum_{t=1}^{T} q_F(j-p_{m',t})\frac{v_{m'}}{d_{m',t}}b_{m',t}(j)\left(N_{m'}(j)-(s_{m'}(j)+s_{m',1}(j)+\ldots+s_{m',T}(j))+1\right)p_{m',t}
\end{aligned}
\tag{6}
$$

for $j = 1, \ldots, P$, where

$$b_{m'}(j) = \begin{cases} 1 \ \text{if} \ (1 \leq j - p_{m'} < P_0 \text{ and } \gamma_{m'} = 1 \text{ and } m' \leq M) \\ \quad \text{or if} \ (1 \leq j < P \text{ and } \gamma_{m'} = 1 \text{ and } m' > M) \\ \quad \text{or if} \ (1 \leq j < P \text{ and } \gamma_{m'} = 0) \\ \quad 0 \ \text{otherwise} \end{cases} \tag{7}$$

$$b_{m',t}(j) = \begin{cases} 1 \ \text{if} \ (P_{t-1} \leq j < P_t \text{ and } \gamma_{m'} = 1 \text{ and } m' \leq M) \\ \quad 0 \ \text{otherwise} \end{cases} \tag{8}$$

and $s_{m'}(j)$, $s_{m',t}(j)$ are the number of active appliances that require $p_{m'}$ and $p_{m',t}$ p.u. respectively.

Proof: see Appendix A

As in the case of the default scenario, the functions $s_{m'}(j)$, $s_{m',t}(j)$ are not known. We propose the following approximation in order to calculate these functions: the number $s_m(j)$ of active appliances, when j p.u. are in use is equal to the mean number of active appliances when Poisson arrivals are considered (i.e. infinite number of appliances):

$$s_{m'}(j) \approx \frac{\left(N_{m'}(j) v_{m'} \cdot d_{m'}^{-1}\right) q_{INF}(j - p_{m'})}{q_{INF}(j)} \tag{9}$$

if ($j \leq P_0 + p_{m'}$ and $\gamma_{m'} = 1$) or ($j \leq P$ and $\gamma_{m'} = 0$) and

$$s_{m't}(j) \approx \frac{\left(N_{m'}(j) v_{m'} d_{m'}^{-1}\right) q_{INF}(j - p_{m',t})}{q_{INF}(j)} \tag{10}$$

if ($P_{t-1} \leq j < P_t$ and $\gamma_{m'} = 1$ and $m' \leq M$). The distribution $q_{INF}(j)$ refers to the distribution of probabilities of the number of p.u. in use, when an infinite number of appliances is assumed to be present in the grid (Eq. (4) in [20]):

$$
\begin{aligned}
& jq_{INF}(j) = \sum_{m'=1}^{2M} R_{m'}(j) d_{m'}^{-1} b_{m'}(j) p_{m'} q_{INF}(j - p_{m'}) + \\
& \sum_{m'=1}^{2M} R_{m'}(j) d_{m'}^{-1} b_{m',t}(j) p_{m',t} q_{INF}(j - p_{m',t})
\end{aligned}
\tag{11}
$$

where the infinite model of Eq. (11) assumes that the arrival rate of requests of type-m appliances is equal to the product $R_{m'}(j) = N_{m'}(j)v_{m'}$ of the number of appliances $N_{m'}(j)$ by the arrival rate $v_{m'}$ per inactive appliance, which are both used in the finite model.

The probability that the total power consumption will exceed P upon the arrival of a compressed power demand for $p_{m',t}$ p.u. is given by:

$$
B_{m',t} = \sum_{j=P-p_{m',t}+1}^{P} \frac{q_F(j)}{Q} \tag{12}
$$

while the probability $B_{m'}$ can be calculated by using Eq. (4) for a power request from an appliance that cannot compress its power demand. Based on both the values of $B_{m',t}$ and $B_{m'}$ we can calculate the minimum value of P so that the outage probability will not exceed a predefined value e. A method for solving the set of Eqs. (5)-(12) is presented in Fig. 2b.

2.3. The Finite Delay Request Scenario

The Finite Delay Request Scenario (FDRS) requires the presence of up to M buffers installed in the CLC, one for each type of appliance. These buffers are used by the CLC in order to delay power requests that arrive in the CLC when the total number of p.u. in use exceeds a power threshold. The delay duration depends on predefined power thresholds, so that gradual increase of power-request delays is achieved as a function of the current power consumption. After the delay in the buffer a power request instantly attempts to access the system. By delaying the power requests, the final requests' arrival rate to the system is reduced, and during this delay several active appliances terminate their operations; therefore, the probability of reaching high-power consumption states is also reduced.

We assume that the delay that a power request of type m appliances suffers when the current power consumption is $P_{t-1} \leq j < P_t$ is denoted as $\delta_{m,t}$. The values of $\delta_{m,t}$ increase with the increment of the power consumption so that $\delta_{m,1} < \delta_{m,2} < ... < \delta_{m,T}$, while they are chosen based on the ability of an appliance to tolerate delays. For example, water heaters can endure a delay in their operation, while a home entertainment set cannot. For appliances that belong to the latter case, the values of the parameters $\delta_{m,t}$ are equal to zero, i.e. no buffers are reserved for these types of appliances. An example of the application of FDRS to delay-tolerant appliances is illustrated in Fig. 3a, where 4 power thresholds are assumed.

The calculation of the distribution of the probabilities $q_F(j)$ for FDRS is based on the arrival rate of the power requests per inactive appliance at the system. The value of the arrival rate of power requests when the total p.u. in use exceeds a power threshold is a function of the delay that these requests suffer in the buffers. More precisely, we first define the inter-arrival time of the power requests of type-m appliances, per inactive appliance. This time is equal to the inter-arrival time $1/v_m$ per inactive appliance of requests that arrive at the buffer plus the delay $\delta_{m,t}$ that these request suffer at the buffers, when the current power consumption is $P_{t-1} \leq j < P_t$. By reversing the resulting sum, we find the rate $\Lambda_{m,t}$ per inactive type-m appliance that power requests egress the buffer:

$$\Lambda_{m,t} = \frac{v_m}{1 + v_m \delta_m} \tag{13}$$

As in the case of FCDS, consumers have the capability to select whether they agree to postpone their demands; the probability that a consumer will agree to postpone a power request for a type-m appliance when the current power consumption is $P_{t-1} \leq j < P_t$ is denoted as $w_{m,t}$. By considering these probabilities, the assumption of two groups of appliances ("elastic"and "un-elastic") that is used in the FCDS case is also applicable to the FDRS, where "elastic"appliances are able to postpone their requests, while the requests of "un-elastic"appliances are not delayed. Therefore, Eq. (5) that defines the number of appliances $N_{m'}(j)$ for FCDS, is also applied to the FDRS case.

By using the arrival rate per inactive appliance of Eq. (13) and the number of appliances $N_{m'}(j)$ of Eq. (5) we can calculate the distribution $q_F(j)$ of the probabilities that j p.u. are in use for the FDRS, by using the following proposed recursive formula:

$$\begin{gathered} j q_F\left(j\right) = \sum_{m'=1}^{2M} \frac{v_{m'}}{d_{m'}} \left(N_{m'}(j) - s_{m'}(j) + 1\right) c_{m'}(j) p_{m'} q_F\left(j - p_{m'}\right) + \\ \sum_{m'=1}^{2M} \frac{\Lambda_{m',t}}{d_{m'}} \left(N_{m'}(j) - \left(s_{m'}(j) + s_{m',1}(j) + \ldots + s_{m',T}(j)\right) + 1\right) c_{m',t}(j) p_{m'} q_F\left(j - p_{m'}\right) \end{gathered} \tag{14}$$

for $j = 1, \ldots, P$, while

$$c_{m'}(j) = \begin{cases} 1 & \text{if } 1 \leq j - p_{m'} \leq P_0 \\ 0 & \text{otherwise} \end{cases} \tag{15}$$

and

$$c_{m',t}(j) = \begin{cases} 1 \ \text{ if } (\mathrm{P}_{t-1} \leq j - p_{m'} < P_t) \text{ and } (\gamma_{m'} = 1) \text{ and } (m' \leq M) \\ 0 \ \text{ otherwise} \end{cases} \tag{16}$$

Proof: see Appendix B.

The calculation of the number of active appliances $s_{m',t}$ and $s_{m',t}$ is performed by using a similar approximation as the one used in the default scenario and in the FCDS. More precisely, the number of active appliances, when j p.u. are in use is equal to the mean number of active appliances when infinite number of appliances in the grid are assumed. Therefore the number $s_{m,t}(j)$ can be calculated by using Eq. (9) for $j - p_{m'} \leq P_0$, while the number $s_{m',t}(j)$ can be calculated by Eq. (10), where $q_{INF}(j)$ should be replaced by the corresponding distribution of probabilities of the number of p.u. in use, when an infinite number of appliances is assumed to be present in the grid (Eq. (9) in [20]):

$$\begin{aligned} jq_{INF}(j) = \sum_{m'=1}^{2M} R_{m'}(j) v_{m'} d_{m'}^{-1} b_{m'}(j) p_{m'} q_{INF}(j - p_{m'}) + \\ \sum_{m'=1}^{2M} R_{m'}(j) \Lambda_{m',t} d_{m'}^{-1} b_{m',t}(j) p_{m'} q_{INF}(j - p_{m'}) \end{aligned} \tag{17}$$

where $R_{m'}(j) = N_{m'}(j) v_{m'}$. Based on the distribution of Eq. (14) we can calculate the probability that the total power consumption will exceed P_t upon the arrival of a power request, by using Eq. (4). A method for solving the set of Eqs. (13)-(17) is presented in Fig. 3b. It should be noted that if the delay δ_m is set to zero for all M types of appliances, then the arrival rate per inactive appliance is equal to v_m for $j = 1, \ldots, P$ (from Eq. (13)), and the FDRS coincides with the default scenario.

2.4. The Finite Postponement Request Scenario

As in the previous scenarios, the Finite Postponement Request Scenario (FPRS) assumes a finite number of appliances for each one of the M types of appliances. The FPRS assumes that there is a threshold P_2 for the p.u. in use. If this threshold is exceeded upon the arrival of a power request, the user of the corresponding appliance is prompted that the operation of the appliance should be delayed, until the number of p.u. in use drops below a second threshold P_1, with $P_1 < P_2$. When the total number of p.u. in use drops below this second threshold, the power demand will immediately try to access the system. An example of the application of FPRS is illustrated in Fig. 4a. The user can decide whether the operation of the appliance is delayed or not. The probability that the user will accept to delay the operation of the appliance is denoted as w_m, while the probability that the use will refuse is equal to $1-w_m$. Based on these assumptions, we define the arrival rate per inactive type-m appliance $v_{m,n}(j)$ as follows:

$$v_{m,n}(j) = \begin{cases} v_{m,1}(j) = v_m + w_m v_m & \text{if } j \leq P_1 \\ v_{m,2}(j) = v_m & \text{if } \mathrm{P}_1 < j \leq P_2 \\ v_{m,3}(j) = (1 - w_m) v_m & \text{if } j > P_2 \end{cases} \tag{18}$$

Based on Eq. (18) we can calculate the distribution of the probabilities

$q_F(j)$ by using the following proposed recursive formula:

$$jq_F\left(j\right) = \sum_{m=1}^{M} v_{m,1} d_m^{-1} \left(S_m - s_m(j) + 1\right) c_{m,1}(j) p_m q_F\left(j - p_m\right) + \sum_{m=1}^{M} \sum_{n=2}^{3} v_{m,n} d_m^{-1} \left(S_m - (s_m(j) + s_{m,2}(j) + s_{m,3}(j)) + 1\right) c_{m,n}(j) p_m q_F\left(j - p_m\right) \quad (19)$$

for $j = 1, \ldots, P$. Also,

$$c_{m,1}(j) = \begin{cases} 1 \text{ if } 0 \leq j \leq P_1 + p_m \\ 0 \text{ otherwise} \end{cases} \quad (20)$$

$$c_{m,2}(j) = \begin{cases} 1 \text{ if } P_1 + p_m < j \leq P_2 + p_m \\ 0 \text{ otherwise} \end{cases} \quad (21)$$

$$c_{m,3}(j) = \begin{cases} 1 \text{ if } P_2 + p_m < j \leq P \\ 0 \text{ otherwise} \end{cases} \quad (22)$$

Proof: see Appendix C.

As in the previous scenarios, the number of active appliances is approximated by the mean number of active appliances when an infinite number of appliances are present in the grid. Therefore, the functions $s_m(j)$, $s_{m,2}(j)$ and $s_{m,3}(j)$ can be derived by using Eq. (8), for $j \leq P_1 + p_m$, $P_1 + p_m < j \leq P_2 + p_m$ and $P_2 + p_m < j \leq P$, respectively, while the distribution $q_{INF}\left(j\right)$ refers to the corresponding distribution of probabilities of the number of p.u. in use, when infinite number of appliances are present in the residential area (Eq. (13) in [20]):

$$jq_{INF}\left(j\right) = \sum_{m=1}^{M} \sum_{n=1}^{3} r_{m,n} d_m^{-1} c_{m,n}(j) p_m q_{INF}\left(j - p_m\right) \quad (23)$$

By using Eq. (19) and Eq. (4) we can calculate the minimum number of p.u. that are required in the grid, so that the maximum outage probability (given by Eq. (4)) will not exceed a predefined value e. Eqs. (18)-(22) can be solved by using a method presented in Fig. 4b. Note that if the probabilities w_m are set to be equal to zero for all M types of appliances, the FPRS coincides with the default scenario.

3. Performance Analysis Of The Proposed Scenarios

3.1. Cost Analysis

The application of a real-time pricing management model is able to improve the efficiency of a smart grid by flattering the load curve. The application of a dynamic power pricing scheme provides an incentive for the customers to reduce their power consumption during peak demand hours. In order for a dynamic pricing pattern to benefit not only the consumer but also the energy provider, it should be defined based on the considered power demand control scenario. In this way, a more balanced charging policy can be applied to customers that decide to postpone or reduce their power demands, while the energy provider will benefit by the reduction of the necessity to activate new power plants.

The *total average energy cost* can be defined through the introduction of a cost function $C(j)$, which is associated to the total number j of p.u. in use. This cost function should be an increasing function, so that the total power cost is enlarged by the increase of the power consumption with a behavior that is in accordance to the applied power demand scenario. The total average energy cost is defined as:

$$A_{C(j)} = \sum_{j=0}^{P} j \cdot q_F(j) \cdot C(j) \tag{24}$$

For the case of the default scenario we can define a simple increasing function in the form of $C(j) = a \cdot j^k$, while for the scheduling scenarios the cost functions should consider the values of the power thresholds. Therefore, in the case of the FCDS, the power demand compression can be rewarded by defining the cost function as $C(j) = b \cdot j^l$ if $j \leq P_0$ and $C(j) = c_t \cdot j^{n_t}$ if $P_{t-1} \leq j < P_t$, where $a \leq b \leq c_1 \leq c_2 \leq ... \leq c_T$ and $k \leq l \leq n_1 \leq n_2 \leq ... \leq n_T$. The values of the parameters c_t, n_t can be determined as a function of the average reduction of the power demands of all M types of appliances, when the power consumption exceeds a power threshold; e.g. if 2 thresholds are applied then $(b/c_1,\ l/n_1) \sim \mathrm{E}(p_m/p_{m,1})$ and $(c_1/c_2,\ \mathrm{n}_1/n_2) \sim \mathrm{E}(p_{m,1}/p_{m,2})$. An analogous cost function can be defined for the case of the FDRS, where the values of the parameters c_t, n_t are functions of the average delay of requests of all M types of appliances, i.e. if 2 thresholds are applied then $(b/c_1,\ l/n_1) \sim \mathrm{E}(1/r_{m,t})$ and $(c_1/c_2,\ \mathrm{n}_1/n_2) \sim \mathrm{E}(1/r_{m,t})$. Finally, for the case of the FPRS the cost function should be a function of the thresholds P_1 and P_2, therefore:

$$C(j) = \begin{cases} b \cdot j^l & \text{if } \ j \leq P_1 \\ c \cdot j^u & \text{if } \ P_1 < j \leq P_2 \\ d \cdot j^s & \text{if } \ j > P_2 \end{cases} \tag{25}$$

where $a \leq b \leq c \leq d$ and $k \leq l \leq u \leq s$.

3.2. Social Welfare

The social welfare can be defined as the total power cost to the consumers minus the total power generation cost [25]. A generation cost function should take into account not only the production cost, but also the no-load cost and the start-up cost [26]. The no-load cost refers to the cost that is incurred whenever a generator is online but idle, while the start-up cost represents the cost required for a generating unit to shift from the OFF state to the ON state. By considering that G generators are connected to the residential area under study, the total generating cost function can be defined as:

$$GC(j) = \sum_{i=1}^{G} \left(\alpha_i j_i^{\kappa_i} + \beta_i j_i^{\lambda_i} + \zeta_i \eta_i f_i(j) + \xi_i \theta_i g_i(j) \right) \tag{26}$$

where α_i and β_i are constants that represent the power production cost of generating j p.u. in unit i ($i = 1, \ldots, G$), ζ_i is a flag, which is set to 0 or 1 if the generating unit i is OFF or ON respectively, and ξ_i is a flag that takes the value 1 when the generating unit i shifts from state OFF to state ON and the value 0 when the unit moves from state ON to state OFF. These two flags change their values depending on the total requested p.u.: in peak-demand hours additional generating units are turned on in order to satisfy the increased power demands. Furthermore, $\eta_i f_i(j)$ and $\theta_i g_i(j)$ denote the no-load and start-up cost, respectively, while the number j of the generating p.u. is the sum of the generating p.u. in each active generating unit.

Having determined the total generating cost function we can define the *total average social welfare* as:

$$SW_{C(j),\,GC(j)} = \sum_{j=0}^{P} j \cdot q_F(j) \cdot (C(j) - GC(j)) \tag{27}$$

4. Evaluation and Discussion

The evaluation of the proposed analytical models for each scenario is performed by comparing analytical results from the proposed models with corresponding results from simulation, as well as with analytical results from [20]. To this end, we assume a residential area with 50 residences. Each residence is equipped with the same 10 appliances; therefore the number of type-m appliance in this area is S_m=50. The 10 types of appliances are: 1) electric stove, 2) laundry pair, 3) water heater, 4) dishwasher, 5) refrigerator, 6) air condition, 7) home office set, 8) entertainment set, 9) lighting and 10) plug-in hybrid electric vehicle (PHEV). The power demands and the operational times of the appliances are listed in Table 1. These values are derived by taking into account the typical power consumption of a residence and by assuming that 1 p.u. = 100 Watt. It should be noted that the power demands of some appliances (e.g. electric stove, air condition, PHEV, etc.) are usually not constant during their entire operational time. However, these appliances can either request the maximum demand for the entire operational duration, or schedule multiple requests with different constant demands each time, over the appliance operational duration. Also, we use the same set of appliances and with the same power demands as in the case of [20], in order to compare the analytical results of the two cases and prove that the proposed finite algorithms are more accurate than the corresponding models in [20].

For the evaluation of the proposed analytical models we built an object-oriented simulator using the C++ programming language. The simulator creates 3×10^6 events based on random numbers for the power requests, while a stabilization time that corresponds to the first 10^5 events is assumed, so that the simulator reaches the steady state. Simulation results are obtained as mean values from 15 simulation iterations, each one with a different seed, while 95% reliability ranges are presented. It should be noted that simulation results from each simulation run are obtained in about 14 min. in average, which is a significantly higher time compared to 2.7 s. in average required in order to obtain the analytical results from the proposed formulas. This fact proves the effectiveness of the proposed analysis, especially when near real-time scheduling decisions are required. In what follows, the proposed analytical models are referred as *finite models* due to the assumption of a finite number of appliances, while the models from [20] are referred as *infinite models*, since the models in [20] assume an infinite number of appliances in the residential area.

For the evaluation of the proposed analytical models we initially consider the default scenario, where no energy or task scheduling occurs. In Fig. 5 we present analytical and simulation peak-demand results for the default scenario from the proposed finite model, together with analytical results from the infinite model of [20]. In order to provide a fair comparison between the proposed analysis and the analysis of [20], we assume that the arrival rate in the infinite model is equal to the product of the number of appliances to the arrival rate in the finite model, or $\lambda_m = S_m v_m$, where λ_m is the arrival rate in the infinite model. This assumption is used in order to consider the same number of power-request arrivals per unit time for the two models. For presentation purposes, we consider the same arrival rate for all appliances; evidently, since the proposed analytical model includes the power-requests arrival rates in a parametric way, any arrival-rate set may be applied. The comparison between analytical and simulation results reveal the satisfactory accuracy of the finite model. Moreover, Fig. 5 shows that serious overestimations of the peak demand occur under the infinite model; this fact proves the necessity for the application of an analytical model that assumes a finite population of appliances, as the models that are presented in the current paper. It should be also pointed out that the analytical results of Fig. 5 are exactly the same with the analytical results obtained by considering that 1 p.u.=0.01 W, without a significant increase of the computation time , due to the use of recursive formulas.

The evaluation of the analytical models for the scheduling scenarios is performed by considering two combined case studies, which are based on the case studies used in [20], so that both energy scheduling and task scheduling appliances are considered. Specifically, we categorize the aforementioned appliance types into three sets: i) the first set comprises of appliances that are able to compress their demands (laundry pair, water heater, air-condition), ii) in the second set we consider appliances that are tolerant to request postponements (electric stove, dishwasher, PHEV), while, iii) appliances that belong to the third set are not participating in any scheduling scheme (refrigerator, home office set, entertainment set, lighting). In the first case study, the energy scheduling appliances together with refrigerator and home-office set are applied to the FCDS, while the task scheduling appliances together with entertainment set and lighting are applied to the FDRS. The second case study is the same as the first case; however FDRS is replaced by the FPRS. It should be noted that appliances that are not participating in any scheduling scheme can be applied to any of FCDS, FDRS or FPRS, since the corresponding analytical models support non-scheduled appliances.

In Fig. 6 we evaluate the performance of the first case study (FCDS and FDRS) by presenting analytical and simulation results for peak demand versus the power-requests' arrival rate. In the same figure we present analytical results of the corresponding case study of [20]. Both FCDS and FDRS consider two power thresholds, which are set to 60% and 75% of the peak demand, respectively. Under FCDS, consumers are prompted to reduce their power demands by 15% and at the same time expand their operational times by the same percentage, when the current power consumption exceeds the first power threshold, while these values are both changed to 25%, when power consumption exceeds the second threshold. For the FDRS case, when the power consumption exceeds the first and the second threshold power requests are delayed for 4 and 8 min, respectively. Furthermore, in both FCDS and FDRS the percentage of consumers that agree to participate in the program is 60%, for the first threshold, and 70% for the second threshold; this participation rate increase is due to more encouraging incentives that are offered to consumers, when the total power consumption is significant. The results of Fig. 6 reveal the satisfactory accuracy of the proposed analysis. We also observe that if we consider the infinite case of [20], serious overestimations of the peak demand occur (average difference 26.5%, minimum difference 19.8% and maximum difference 33.1%).

In Fig. 7 we provide analytical and simulation peak-demand results under the FCDS-FPRS study case. The FPRS results are obtained by considering that the two thresholds P_1 and P_2 are set to the 60% and 75% of the peak demand, respectively, while the participation rate is set to 70%. The results of the FCDS are obtained by using the same parameter values as the ones that are used for the derivation of the results of Fig. 6. We also provide corresponding analytical results from the infinite model, which are derived by assuming that the arrival rate is equal to the product of the number of appliances to the arrival rate per inactive appliance in the finite model. The comparison of analytical and simulation results reveal that the accuracy of the proposed model is quite satisfactory. We also observe that, as in the FCDS-FDRS study case, the infinite model overestimates the peak demand (average difference 21.8%, minimum difference 17.0% and maximum difference 27.1%).

It is important to mention that the total number of appliances that are installed in the residential area plays an important role for the determination of the total number of requested p.u. The effect of the population of appliances on the total number of requested p.u. is shown in Fig. 8, where analytical results for the four scenarios are presented. We consider that in each point (but the last) in the x-axis of Fig. 8 the product (Number of appliances) by (arrival rate per inactive appliance) is kept constant and equal to 0.4 requests per minute for every type of appliance. In order to provide a fair comparison between the different scenarios, we consider a single power threshold for FCDS and FDRS, which is equal to 60% of the peak demand, so that a single value of the participation rate is assumed, as in the case of FPRS; the participation rate is assumed to be equal to 70% for FCDS, FDRS and FPRS. Under FCDS, the power compression is equal to 25%, while under FDRS power requests are delayed for 10 minutes. The results that correspond to the infinite population (last point in the x-axis of Fig. 8) are derived by the corresponding analytical results of [20]. We observe that when the population of appliances increases, the total number of requested p.u. also increases. This behavior is explained by the fact that when a large number of appliances are installed in the residential area, the percentage of idle appliances is higher; therefore the number of requests that arrive from these inactive appliances is higher and more p.u. are necessary for the satisfaction of all power requests. We also observe that the best performance is achieved by the application of the FDRS, in terms of lower number of requested p.u.. Evidently, the difference between the four scenarios is a function of the values of the parameters that are selected for each scenario. Nevertheless, the results of Fig. 8 indicate the significant advantages of the proposed finite models over the infinite models of [20], especially when they are applied to small appliances' population cases.

Finally we demonstrate the influence of the application of the power control scenarios on the total average social welfare by using the same parameter values that were used in order to derive the results in Fig. 8. In order to provide a fair comparison of the performance of the four scenarios we assume the same generating cost function for all scenarios, which is given by Eq. (25) and by using the following assumptions: the residential area under study is connected to two generating units: the primary unit, which produces up to 2600 p.u. and a secondary unit which is activated when the total power consumption exceeds a single power threshold of 2600 p.u.. For the two generating units the power production parameters are α_1=2, β_1=3, κ_1=2, λ_1=2, α_2=5, β_2=20, κ_2=3, λ_2=2. Furthermore, the no-load cost and start-up cost parameters of the two units are η_1=2, θ_1=2, η_2=5 and θ_2=4 and the corresponding functions are $f_1(j) = 10^5$, $g_1(j) = 5 \times 10^4$ for $j \leq 2600$ and $f_2(j) = 8 \times 10^5$, $g_2(j) = 10^5$ for $j > 2600$. These values were chosen in order to show that the generating cost is significantly increased by the activation of the second generating unit. For the case of the default scenario the cost function is $C(j) = 5 \cdot j^3$. The cost function that corresponds to the FCDS takes into account the reduction of power demands by 20%, when the total power consumption exceeds the threshold P_0, by reducing the parameter b by 30%, compared to the parameter c which is equal to 5 (as in the case of the default scenario); therefore the cost function is $C(j) = 3.5 \cdot j^3$ if $j \leq P_0$ and $C(j) = 5 \cdot j^3$ if $j > P_0$. For the case of the FDRS the same cost function is applied. Finally, for the case of the FPRS the cost function is $C(j) = 3 \cdot j^3$ if $j \leq P_1$, $C(j) = 4 \cdot j^3$ if $P_1 < j \leq P_2$, and $C(j) = 5 \cdot j^3$ if $j > P_2$. In Fig. 9 and Fig. 10 we present analytical results for the total average cost and the total average social welfare, respectively, for the four power demand control scenarios versus the total arrival rate. As it was expected, under the default scenario the total average cost is higher compared to the corresponding values of the other scenarios, since no demand compression or request delay occurs. The average reduction of the total average cost for FCDS, compared to the default scenario is 41.6%, for FPRS the average reduction is 39.3% and for FDRS the average reduction is 17.9%. On the other hand, as the results of Fig. 10 reveal, under all scenarios the total average social welfare is a concave function of the power-requests' arrival rate: when the arrival rate increases, then the welfare also increases, since the total electricity cost is increased. However, after a certain arrival-rate point, the generation cost is significant (due to the activation of the secondary generation unit) and the social welfare decreases. It should be noted that the maximum value of the average welfare is positioned at different arrival-points for each scheduling scenario. This is due to the fact that under the FCDS, FDRS or FPRS the total power consumption exceeds the power threshold that is assumed for the activation of the secondary generation unit (which results in higher generation costs) for higher arrival-rate values, compared to the default scenario; these values are different for each scenario, due to the dissimilar effect of each scenario on the power consumption reduction. Consequently, the proposed scenarios can be considered as a solution for restraining the necessity for the activation of supplementary power plants to meet peak demand.

5. Conclusion

We propose more realistic and accurate analytical models for the determination of the peak demand in a residential area, under four power demand control scenarios. The proposed analysis is based on the assumption of finite number of appliances in the area under study, which is expressed by a quasi-random process for the arrivals or power requests. For each scenario a recursive formula is derived, in order to efficiently calculate the peak demand as a function of the number of appliances. The accuracy of the proposed models is quite satisfactory, as it is verified by simulation. We also compare results from our proposed analysis with corresponding results from

[20], in order to reveal the necessity of an analytical model that assumes a finite number of appliances. Furthermore, we associate each scenario with appropriate real-time pricing procedures, in order to provide incentives to customers to compress or delay their power demands and we calculate the social welfare. The results of the proposed models are derived in a small computational time, compared to simulations; this fact allows the application of the proposed models to DR programs that require near real-time decisions.

Acknowledgment

This work has been funded by the E2SG project, an ENIAC Joint Undertaking under grant agreement No. 296131 and by the project AGAUR (2014SGR 1551).

Appendix A. Proof of the recursive formula of Eq. (6)

In order to derive Eq. (6) we initially consider the case of a single power threshold P_0, and we construct the one dimensional Markov chain with the state transition diagram of Fig. 11a. In this Markov chain each state j represents the number of p.u. in use, for $j - p_{m'} \leq P_0$ and shows the transitions when a type-m' appliance is activated and deactivated. If we assume that $s_{m'}(j)$ appliances of type m' are active in state j, then the number of inactive appliances of the same type in state j is $(N_{m'}(j) - s_{m'}(j))$ and the number of inactive appliances in state $j - p_{m'}$ is $(N_{m'}(j) - (s_{m'}(j) - 1)) = (N_{m'}(j) - s_{m'}(j) + 1)$; therefore, power requests will arrive from this set of appliances. Based on this analysis we define the transition rates in Fig. 11a, while the local balance equation of the state transition diagram of Fig. 11a is:

$$\begin{aligned} q_F(j-p_{m'})v_{m'}\left(N_{m'}(j)-s_{m'}(j)+1\right) &= q_F(j)y_{F,m'}(j)d_{m'} \Leftrightarrow \\ q_F(j-p_{m'})\tfrac{v_{m'}}{d_{m'}}\left(N_{m'}(j)-s_{m'}(j)+1\right)p_{m'} &= q_F(j)y_{F,m'}(j)p_{m'} \end{aligned} \tag{A.1}$$

for $j - p_{m'} \leq P_0$ and $m' = 1, \ldots, 2M$. The function $y_{F,m'}(j)$ is the mean number of appliances in use in the grid that require $p_{m'}$ p.u., when the total number of p.u. in use is $j \leq P_0 + p_{m'}$.

We also construct the one dimensional Markov chain of the system with the state transition diagram of Fig. 11b, where each state j represents the number of p.u. in use, for $j - p_{m'} > P_0$. The number of appliances that are active in state $j > P_0$ is equal to $s_{m'}(j) + s_{m',1}(j)$; $s_{m'}(j)$ active appliances that were accepted for service when the system was in any state below P_0 and $s_{m',1}(j)$ active appliances when the system was in state above P_0. Therefore, the number of inactive appliances in state $j - p_{m'}$ is $(N_{m'}(j) - (s_{m'}(j) + s_{m',1}(j)) + 1)$, therefore power requests will arrive from this set of appliances. The local balance equation of the state transition diagram of Fig 11b is:

$$\begin{aligned} q_F(j-p_{m',1})v_{m'}\left(N_{m'}(j) -)(s_{m'}(j) + s_{m',1}(j)) + 1\right) &= q_F(j)y_{F,m',1}(j)d_{m',1} \Leftrightarrow \\ q_F(j-p_{m',1})\tfrac{v_{m'}}{d_{m',1}}\left(N_{m'}(j)-(s_{m'}(j)+s_{m',1}(j))+1\right)p_{m',1} &= q_F(j)y_{F,m',1}(j)p_{m',1} \end{aligned} \tag{A.2}$$

for $j - p_{m',1} > P_0$ and $m' = 1, \ldots, 2M$, where $s_{m',1}(j)$ is the number of active appliances of type-m' that have compressed their demands. Also, the function $y_{F,m',1}(j)$ is the mean number of appliances in use in the grid that require $p_{m',1}$ p.u., when the total number of p.u. in use is $j > P_0 + p_{m',1}$.

By considering the entire set $2M$ of appliances types, Eq. (A-1) is transformed to:

$$\begin{aligned} &\sum_{m'=1}^{2M} q_F(j-p_{m'})\tfrac{v_{m'}}{d_{m'}}\left(N_{m'}(j)-s_{m'}(j)+1\right)p_{m'} = \\ &q_F(j)\sum_{m'=1}^{2M} y_{F,m'}(j)p_{m'}, \quad j \leq P_0 - p_{m'} \end{aligned} \tag{A.3}$$

Also, from Eq. (A-2) and for all $2M$ types of appliances, we obtain:

$$\begin{aligned} &\sum_{m'=1}^{2M} q_F(j-p_{m',1})\tfrac{v_{m'}}{d_{m',t}}\left(N_{m'}(j)-(s_{m'}(j)+s_{m',1}(j))+1\right)p_{m',1} = \\ &q_F(j)\sum_{m'=1}^{2M} y_{F,m',1}(j)p_{m'}, \quad j > P_0 - p_{m',1} \end{aligned} \tag{A.4}$$

In order to derive the total number j of the p.u. in use in any state $0 \leq j \leq P$ we sum the products of the mean number of appliances in use by the number of p.u. that these appliances demand, for all $2M$ power levels:

$$j = \left[\sum_{m'=1}^{2M} y_{F,m'}(j)p_{m'} + \sum_{m'=1}^{2M} y_{F,m',1}(j)p_{m',1}\right] \tag{A.5}$$

Therefore, in order for the summation of the Right Hand Side (RHS) of Eq. (A-3) to be equal to j, we have to assume that $y_{F,m',1}(j) \cong 0$ for $j \leq P_0 - p_{m'}$. Similarly, in order for the summation of RHS of Eq. (A-4) to be equal to j, we have to assume that $y_{F,m'}(j) \cong 0$ for $j > P_0 - p_{m,1}$. These two assumptions should be considered at the expression of the rate that the system jumps from any state $j - p_{m'}$ (or $j - p_{m',t}$) to state j. By summing up side by side Eq. (A-3) and Eq. (A-4), by applying these two assumptions and by using Eq. (A-5), we obtain the following equation:

$$\sum_{m'=1}^{2M} \tfrac{v_m}{d_m} \left(N_{m'}(j) - s_{m'}(j) + 1\right) b_{m'}(j) p_{m'} q_F \left(j - p_{m'}\right) +$$
$$\sum_{m'=1}^{2M} \tfrac{v_m}{d_{m',1}} \left(N_{m'}(j) - (s_{m'}(j) + s_{m',1}(j)) + 1\right) b_{m',1}(j) p_{m',1} q_F \left(j - p_{m',1}\right) = j q_F \left(j\right) \tag{A.6}$$

for $j = 1, ..., P$. The functions $b_{m'}(j)$ and $b_{m',1}(j)$ express the aforementioned assumptions for the functions $y_{F,m'}$ and $y_{F,m',1}$ and they are defined as follows:

$$b_{m'}(j) = \begin{cases} 1 \ \text{ if } \ (1 \leq j - p_{m'} < P_0 \text{ and } \gamma_{m'} = 1 \text{ and } m' \leq M) \\ \quad \text{or if } \ (1 \leq j < P \text{ and } \gamma_{m'} = 1 \text{ and } m' > M) \\ \quad \text{or if } \ (1 \leq j < P \text{ and } \gamma_{m'} = 0) \\ 0 \quad \text{otherwise} \end{cases} \tag{A.7}$$

$$b_{m',1}(j) = \begin{cases} 1 \ \text{ if } \ (j > P_0 + p_{m',1} \text{ and } \gamma_{m'} = 1 \text{ and } m' \leq M) \\ 0 \ \text{ otherwise} \end{cases} \tag{A.8}$$

The consideration of T thresholds affects the transition rates when $j > P_0 + p_{m',t}$ $(t = 1, \ldots, T)$. Precisely, by considering T thresholds P_0, P_1,. . ., P_{T-1}, the local balance equation when $j \leq P_0 - p_{m'}$ remains the same as the single-threshold case and is given by Eq. (A-1), while the local balance equation when $P_{t-1} \leq j - p_{m',t} < P_t$ is given by:

$$q_F(j - p_{m',t}) v_{m'} \left(N_{m'}(j) - (s_{m'}(j) + s_{m',1}(j) + ... + s_{m',T}(j)) + 1\right) =$$
$$= q_F(j) y_{F,m',t}(j) d_{m',t} \Leftrightarrow$$
$$q_F(j - p_{m',t}) \tfrac{v_{m'}}{d_{m',t}} \left(N_{m'}(j) - (s_{m'}(j) + s_{m',1}(j) + ... + s_{m',T}(j)) + 1\right) p_{m',t} =$$
$$= q_F(j) y_{F,m',t}(j) p_{m',t} \tag{A.9}$$

By applying Eq. (A-9) for all $2M$ appliances' types and T thresholds, we obtain:

$$\sum_{m'=1}^{2M}\sum_{t=1}^{T} q_F(j-p_{m',t})\frac{v_{m'}}{d_{m',t}}(N_{m'}(j)-(s_{m'}(j)+s_{m',1}(j)+...+s_{m',T}(j))+1)p_{m',t}= \\ = q_F(j)\sum_{m'=1}^{2M}\sum_{t=1}^{T} y_{F,m',t}(j)p_{m',t} \tag{A.10}$$

Since the total number j of p.u. in use is the sum of the products of the mean number of appliances in use by the number of p.u. that these appliances request:

$$j=\left[\sum_{m'=1}^{2M} y_{F,m'}(j)p_{m'}+\sum_{m'=1}^{2M} y_{F,m',1}(j)p_{m',1}+...+\sum_{m'=1}^{2M} y_{F,m',T}(j)p_{m',T}\right] \tag{A.11}$$

we apply the following approximations: i) $y_{F,m'}(j) \cong 0$ for $j > P_0 - p_{m'}$, in order for the right hand side of Eq. (A-3) to be equal to $jq_F(j)$, and ii) $y_{F,m',t}(j) \cong 0$ outside the region $[P_{t-1}, P_t]$, so that the right hand side of Eq. (A-10) is equal to $jq_F(j)$. By summing up size by size Eq. (A-3) and Eq. (A-10) we derive Eq. (6), where the aforementioned approximations are expressed by Eq. (7) and Eq. (8), respectively.

Appendix B. Proof of the recursive formula of Eq. (14)

By following the same procedure as the one followed for the proof of Eq. (6), we define the local balance equations from the corresponding state transition diagrams, for $j - p_{m'} \leq P_0$:

$$\begin{aligned} &q_F(j-p_{m'})\left(N_{m'}(j)-s_{m'}(j)+1\right)v_{m'} = q_F(j)y_{F,m'}(j)d_{m'} \Leftrightarrow \\ &q_F(j-p_{m'})\left(N_{m'}(j)-s_{m'}(j)+1\right)\tfrac{v_{m'}}{d_{m'}}p_{m'} = q_F(j)y_{F,m'}(j)p_{m'} \end{aligned} \tag{B.1}$$

where $y_{F,m'}(j)$ is the mean number of appliances that require $p_{m'}$ p.u. when j p.u. are in use in the system. Also, by considering the T thresholds, the local balance equation when $P_{t-1} \leq j - p_{m'} < P_t$ is:

$$\begin{aligned} &q_F(j-p_m)\Lambda_{m',t}\left(N_{m'}(j)-(s_{m'}(j)+s_{m',1}(j)+...+s_{m',T}(j))+1\right) = \\ &= q_F(j)y_{F,m',t}(j)d_{m'} \Leftrightarrow \\ &q_F(j-p_{m'})\tfrac{\Lambda_{m',t}}{d_{m'}}\left(N_{m'}(j)-(s_{m'}(j)+s_{m',1}(j)+...+s_{m',T}(j))+1\right)p_{m'} = \\ &= q_F(j)y_{F,m',t}(j)p_{m'} \end{aligned} \tag{B.2}$$

since the power-request arrival rate when the current power consumption is $P_{t-1} \leq j - p_{m'} < P_t$ is reduced from $v_{m'}$ to $\Lambda_{m',t}$. Eq. (B-1) and Eq. (B-2) are converted to the following two equations, respectively, by considering all $2M$ types of appliances:

$$\begin{aligned} &\sum_{m'=1}^{2M} q_F(j-p_{m'})\tfrac{v_{m'}}{d_{m'}}\left(N_{m'}(j)-s_{m'}(j)+1\right)p_{m'} = \\ &q_F(j)\sum_{m'=1}^{2M} y_{F,m'}(j)p_{m'}, \quad j \leq P_0 - p_{m'} \end{aligned} \tag{B.3}$$

$$\begin{aligned} &\sum_{m'=1}^{2M}\sum_{t=1}^{T} q_F(j-p_{m'})\tfrac{\Lambda_{m',t}}{d_{m'}}\left(N_{m'}(j)-(s_{m'}(j)+s_{m',1}(j)+...+s_{m',T}(j))+1\right)p_{m'} = \\ &= q_F(j)\sum_{m'=1}^{2M}\sum_{t=1}^{T} y_{F,m',t}(j)p_{m'} \end{aligned} \tag{B.4}$$

Therefore, Eq. (14) can be derived by following the same procedure as the one used for the proof of Eq. (6), while also considering the following assumptions: i) $y_{F,m'}(j) \cong 0$ for $j > P_0 - p_{m'}$, and ii) $y_{F,m',t}(j) \cong 0$ outside the region $[P_{t-1}, P_t]$; these assumptions are expressed by Eq. (15) and Eq. (16), respectively.

Appendix C. Proof of the recursive formula of Eq. (19)

By following the same procedure as the one followed for the proof of Eq. (6), we define the local balance equations from the corresponding state transition diagrams, for $j - p_m \leq P_0$:

$$\begin{aligned} &q_F(j-p_m)\left(N_m(j) - s_m(j) + 1\right) v_{m,1} = q_F(j) y_{F,m,1}(j) d_m \Leftrightarrow \\ &q_F(j-p_m)\left(N_m(j) - s_m(j) + 1\right) \tfrac{v_{m,1}}{d_m} p_m = q_F(j) y_{F,m,1}(j) p_m \end{aligned} \tag{C.1}$$

where $y_{F,m,1}(j)$ is the mean number of appliances that require $p)m$ p.u. when j p.u. are in use in the system. Also, for $P_1 + p_m < j \leq P_2 + p_m$, and for $P_2 + p_m < j \leq P$, the corresponding local balance equations are respectively given by:

$$\begin{aligned} &q_F(j-p_m)\left(S_m - s_{m,2}(j) + 1\right) v_{m,2} = q_F(j) y_{F,m,2}(j) d_m \Leftrightarrow \\ &q_F(j-p_m)\left(S_m - s_{m,2}(j) + 1\right) \tfrac{v_{m,2}}{d_m} p_m = q_F(j) y_{F,m,2}(j) p_m \end{aligned} \tag{C.2}$$

$$\begin{aligned} &q_F(j-p_m)\left(S_m - s_{m,3}(j) + 1\right) v_{m,3} = q_F(j) y_{F,m,3}(j) d_m \Leftrightarrow \\ &q_F(j-p_m)\left(S_m - s_{m,3}(j) + 1\right) \tfrac{v_{m,3}}{d_m} p_m = q_F(j) y_{F,m,3}(j) p_m \end{aligned} \tag{C.3}$$

where $y_{F,m,2}(j)$ and $y_{F,m,3}(j)$ denote the mean number of appliances that require p_m p.u. when j p.u. are in use in the grid, for $P_1 + p_m < j \leq P_2 + p_m$, and for $P_2 + p_m < j \leq P$, respectively, while $s_{m,2}(j)$ and $s_{m,3}(j)$ are the mean number of appliances that are activated when the total number of p.u. in use upon the arrival of the power request is $P_1 + p_m < j \leq P_2 + p_m$, and $P_2 + p_m < j \leq P$, respectively. By using Eq. (C-1), Eq. (C-2) and Eq. (C-3) and by summing up for all M power levels, we obtain:

$$
\begin{aligned}
&\sum_{m=1}^{M} q_F(j - p_m)\tfrac{v_{m,1}}{d_m}\left(S_m - s_m(j) + 1\right) p_m = \\
&q_F(j) \sum_{m=1}^{M} y_{F,m,1}(j) p_m, \quad j \leq P_1 - p_m \\
&\\
&\sum_{m=1}^{M} q_F(j - p_m)\tfrac{v_{m,2}}{d_m}\left(S_m - s_{m,2}(j) + 1\right) p_m = \\
&q_F(j) \sum_{m=1}^{M} y_{F,m,2}(j) p_m, \quad P_1 - p_m < j \leq P_2 - p_m \\
&\\
&\sum_{m=1}^{M} q_F(j - p_m)\tfrac{v_{m,3}}{d_m}\left(S_m - s_{m,3}(j) + 1\right) p_m = \\
&q_F(j) \sum_{m=1}^{M} y_{F,m,3}(j) p_m, \quad P_2 - p_m < j \leq P
\end{aligned}
\tag{C.4}
$$

As in the case of the FCDS and FDRS, we need to assume that $y_{F,m,1}(j) \approx 0$ for $j > P_1 - p_m$, $y_{F,m,2}(j) \approx 0$ outside the region $P_1 - p_m < j \leq P_2 - p_m$ and that $y_{F,m,3}(j) \approx 0$ for $j < P_2 - p_m$. Due to these three assumptions the rate by which the system jumps from any state $j - p_m$ to state j can be generalized to $(S_{m,t} - (s_{m,t}(j) + s_{m,2,t}(j) + s_{m,3,t}(j)) + 1)$ for any system state; this rate should be considered in Eq. (C-1), Eq. (C-2) and Eq. (C-3), in order to have a generalized expression of the these rates. By using the three assumptions and by summing up side by side the three equations of Eq. (C-4) we derive Eq. (19), while these assumptions are expressed by Eq. (20), Eq. (21), and Eq. (22), respectively.

References

[1] G. W. Arnold, Challenges and opportunities in smart grid: A position article, Proceed. IEEE 99 (16) (2011) 922 – 927.

[2] W. Su, M.-Y. Chow, Computational intelligence-based energy management for a large-scale phev/pev enabled municipal parking deck, Applied Energy 96 (7) (2012) 171 – 182.

[3] M. Wissner, The smart grid – a saucerful of secrets?, Applied Energy 88 (7) (2011) 2509 – 2518.

[4] J. S. Vardakas, N. Zorba, C. V. Verikoukis, A survey on demand response programs in smart grids: Pricing methods and optimization algorithms, IEEE Communications Surveys and Tutorials 17 (1) (2015) 152 – 178.

[5] X. Xue, S. Wang, C. Yan, B. Cui, A fast chiller power demand response control strategy for buildings connected to smart grid, Applied Energy 137 (2015) 77 – 87.

[6] N. Venkatesan, J. Solanki, S. K. Solanki, Residential demand response model and impact on voltage profile and losses of an electric distribution network, Applied Energy 96 (0) (2012) 84 – 91.

[7] P. Faria, Z. Vale, Demand response in electrical power supply: An optimal real time pricing approach, Energy 36 (2011) 5354 – 5374.

[8] M. Parvania, M. Fotuhi-Firuzabad, Demand response scheduling by stochastic scuc, IEEE Transactions on Smart Grid 1 (1) (2010) 88 – 98.

[9] G. Xiong, C. Chen, S. Kishore, A. Yener, Smart (in-home) power scheduling for demand response on the smart grid, in: Innovative smart grid technologies (ISGT), 2011 IEEE PES, 2011.

[10] I. Koutsopoulos, L. Tassiulas, Optimal control policies for power demand scheduling in the smart grid, IEEE J. Sel. Areas Commun. 30 (6) (2012) 1049 – 1060.

[11] J. Valenzuela, P. R. Thimmapuram, J. Kim, Modeling and simulation of consumer response to dynamic pricing with enabled technologies, Applied Energy 96 (2012) 122 – 132.

[12] A. H. Mohsenian-Rad, A. Leon-Garcia, Optimal residential load control with price prediction in real-time electricity pricing environments, IEEE Trans. Smart Grid 1 (2) (2010) 120 – 133.

[13] D. Setlhaolo, X. Xia, J. Zhang, Optimal scheduling of household appliances for demand response, Electric Power Systems Research 116 (2014) 24–28.

[14] D. Setlhaolo, X. Xia, Optimal scheduling of household appliances with a battery storage system and coordination, Energy and Buildings 94 (2015) 61–70.

[15] A. J. Conejo, J. M. Morales, L. Baringo, Real-time demand response model, IEEE Trans. Smart Grid 1 (3) (2010) 236 – 242.

[16] T. Sousa, H. Morais, J. Soares, Z. Vale, Day-ahead resource scheduling in smart grids considering vehicle-to-grid and network constraints, Applied Energy 96 (2012) 183 – 193.

[17] M. Shinwari, A. Youssef, W. Hamouda, A water-filling based scheduling algorithm for the smart grid, IEEE Trans. Smart Grid 3 (2) (2012) 710 – 719.

[18] A. Di Giorgio, F. Liberati, Near real time load shifting control for residential electricity prosumers under designed and market indexed pricing models, Applied Energy 128 (2014) 119 – 132.

[19] S. Borenstein, M. Jaske, A. Rosenfeld, Dynamic pricing, advanced metering, and demand response in electricity markets, Center for the Study of Energy Markets.

[20] J. S. Vardakas, N. Zorba, C. V. Verikoukis, Performance evaluation of power demand scheduling scenarios in a smart grid environment, Applied Energy 142 (2015) 164 – 178.

[21] J. S. Vardakas, N. Zorba, C. V. Verikoukis, Scheduling policies for two-state smart-home appliances in dynamic electricity pricing environments, Energy 69 (0) (2014) 455 – 469.

[22] Energy to the smart grid, `http://www.e2sg-project.eu/`, [Online; Accessed 6 March 2015].

[23] C. Chen, K. Nagananda, G. Xiong, S. Kishore, L. Snyder, A communication-based appliance scheduling scheme for consumer-premise energy management systems, Smart Grid, IEEE Transactions on 4 (1) (2013) 56–65.

[24] G. Stamatelos, V. Koukoulidis, Reservation-based bandwidth allocation

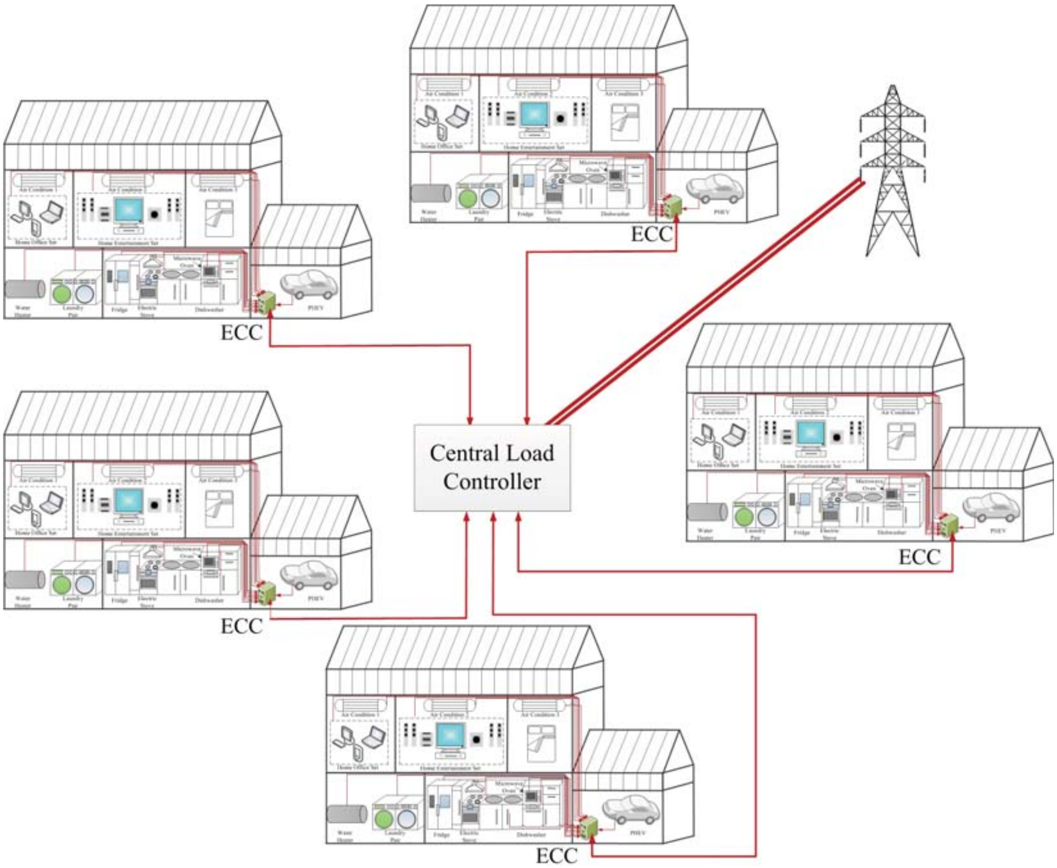

Figure C.1: A typical smart grid infrastructure.

in radio atm network, IEEE/ACM Transactions on Networking 5 (3) (2006) 420 – 428.

[25] D. Veit, A. Weidlich, J. Yao, S. Oren, Simulating the dynamics in two-settlement electricity markets via an agent-based approach, International Journal of Management Science and Engineering Management 1 (2) (2006) 83 – 97.

[26] H. Saadat, Power system analysis, 3rd ed., PSA Publishing, 2010.

Table C.1: Power demands and operational times of the 10 appliances installed in each residence.

appliances	electric stove	laundry pair	water heater	dishwasher	refrigerator	air condition	home office set	entertainment set	lighting	PHEV
power demand p_m (p.u.)	20	15	40	10	6	25	5	7	4	100
operational time d_m^{-1} (min.)	40	30	30	40	60	40	40	50	60	30

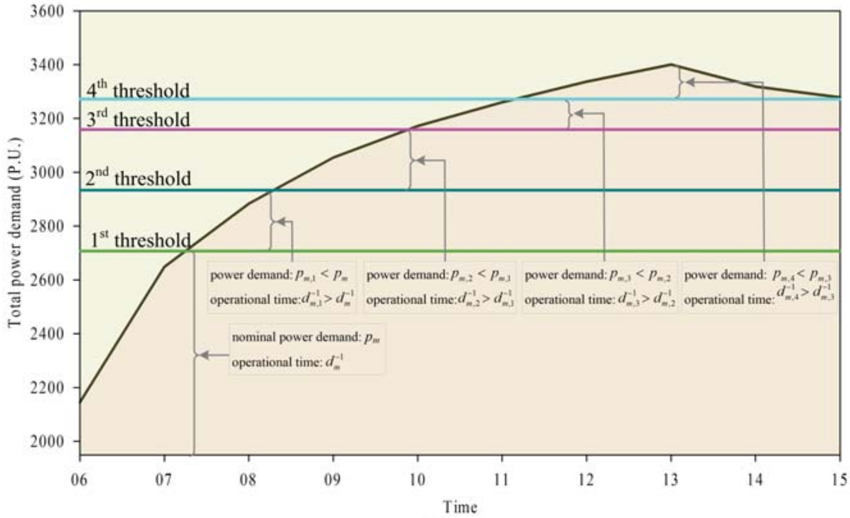

(a)

```
Input: a set of M appliances (S_m, v_m, d_m, p_m, w_m,t, p_m,T, d_m,t), the number of
thresholds T and P_0, P_1,…, P_T.
Initialize: P ← max(p_m), p_m',t=p_m'-M,t, d_m',t=d_m'-M,t,for m' ≥ M.
while (1>0) do
  q_INF(0)=1;
    for j=1 to P do
      for m'=1 to 2M do
        calculate N_m'(j) through (5)
        calculate b_m'(j) for the infinite model through (7)
        for t=1 to T do
          calculate b_m',t(j) for the infinite model through (8)
        end for
      end for
      calculate q_INF(j) through (11)
  end for
  for j=1 to P do
    for m'=1 to 2M do
      calculate s_m'(j) through (9)
      for t=1 to T do
        calculate s_m',t(j) through (10)
      end for
    end for
  end for
  q_F(0)=1;
  for j=1 to P do
      for m'=1 to 2M do
        calculate b_m'(j) for the finite model through (7)
        for t=1 to T do
          calculate b_m',t(j) for the finite model through (8)
        end for
      end for
      calculate q_F(j) through (6)
      Q ← Q+q_F(j)
  end for
  for m'=1 to 2M do
    calculate B_m' through (4)
    for t=1 to T do
      calculate B_m',t through (12)
    end for
  end for
  if max(B_m', B_m',1,…, B_m',T)> e
    P ← P+1;
  else
    break;
  end if
end while
```

infinite model required for the calculation of $s_{m',t}(j)$

finite model

(b)

Figure C.2: (a) Example of the operation of the Finite Compressed Demand Scenario (FCDS), (b) Flowchart of the FCDS.

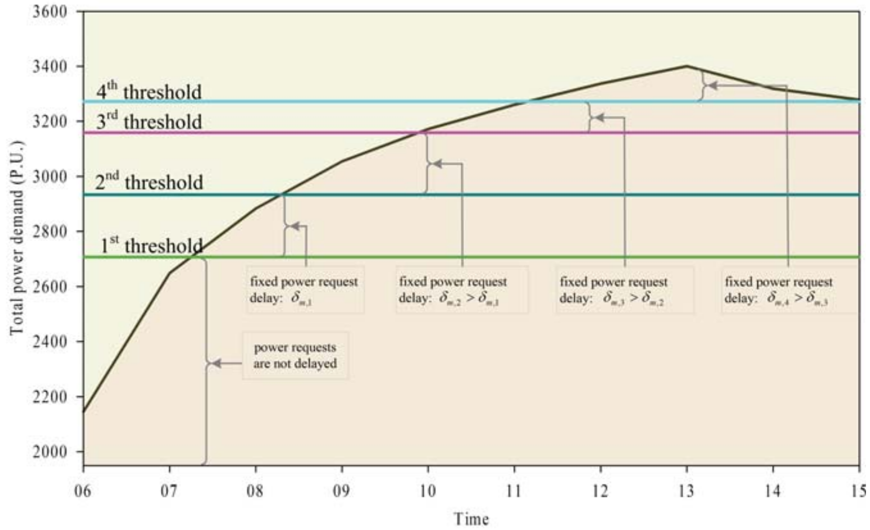

(a)

```
Input: a set of M appliances (Sm, vm, dm, pm, wm,t, δm,T), the number of
thresholds T and P0, P1,…, PT as percentages of P.
Initialize: P ← max(pm), pm',t=pm'-M,t, dm',t=dm'-M,t, for m' ≥ M.
while (1>0) do
  qINF(0)=1;
    for j=1 to P do
      for m'=1 to 2M do
        calculate Nm'(j) through (5)
        calculate the final arrival rate through (13)
        calculate cm'(j) for the infinite model through (15)
        for t=1 to T do
          calculate cm',t(j) for the infinite model through (16)
        end for
      end for
      calculate qINF(j) through (17)
  end for
  for j=1 to P do
    for m'=1 to 2M do
      calculate sm'(j) through (9)
      for t=1 to T do
        calculate sm',t(j) through (10)
      end for
    end for
  end for
  qF(0)=1;
  for j=1 to P do
      for m'=1 to 2M do
        calculate cm'(j) for the finite model through (15)
        for t=1 to T do
          calculate cm',t(j) for the finite model through (16)
        end for
      end for
      calculate qF(j) through (14)
      Q ← Q+qF(j)
  end for
  for m'=1 to 2M do
    calculate Bm' through (4)
  end for
  if max(Bm', Bm',1,…, Bm',T)> e
    P ← P+1;
  else
    break;
  end if
end while
```

infinite model required for the calculation of $s_{m',t}(j)$

finite model

(b)

Figure C.3: (a) Example of the operation of the Finite Delay Request Scenario (FDRS), (b) Flowchart of the FDRS.

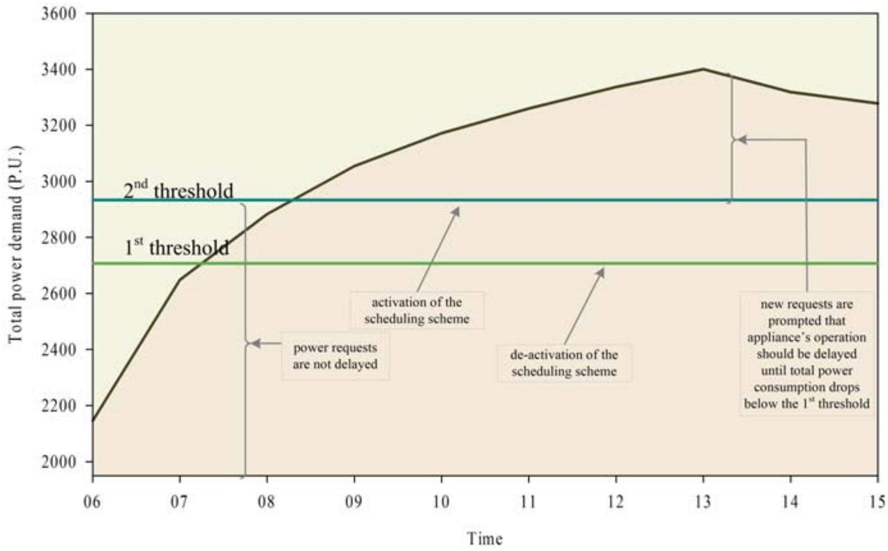

(a)

```
Input: a set of M appliances (Sm, vm, dm, pm, wm,t), and P1, P2, as percentages
of P.
Initialize: P ← max(pm)
while (1>0) do
  qINF(0)=1;
    for j=1 to P do
      for m=1 to M do
        calculate vm,1(j), vm,2(j), vm,3(j)
        for the infinite model through (15)
        calculate cm,1(j) for the infinite model through (20)
        calculate cm,2(j) for the infinite model through (21)
        calculate cm,3(j) for the infinite model through (22)
      end for
      calculate qINF(j) through (23)
  end for
  for j=1 to P do
    for m=1 to M do
      calculate sm(j) through (9)
      for n=2 to 3 do
        calculate sm,n(j) through (10)
      end for
    end for
  end for
  qF(0)=1;
  for j=1 to P do
      for m=1 to M do
        calculate cm,1(j) for the finite model through (20)
        calculate cm,2(j) for the finite model through (21)
        calculate cm,3(j) for the finite model through (22)
      end for
      calculate qF(j) through (19)
      Q ← Q+qF(j)
  end for
  for m'=1 to 2M do
    calculate Bm' through (4)
  end for
  if max(Bm', Bm',1,…, Bm',T)> e
    P ← P+1;
  else
    break;
  end if
end while
```

infinite model required for the calculation of $s_{m',l}(j)$

finite model

(b)

Figure C.4: (a) Example of the operation of the Finite Postponement Request Scenario (FPRS), (b) Flowchart of the FPRS.

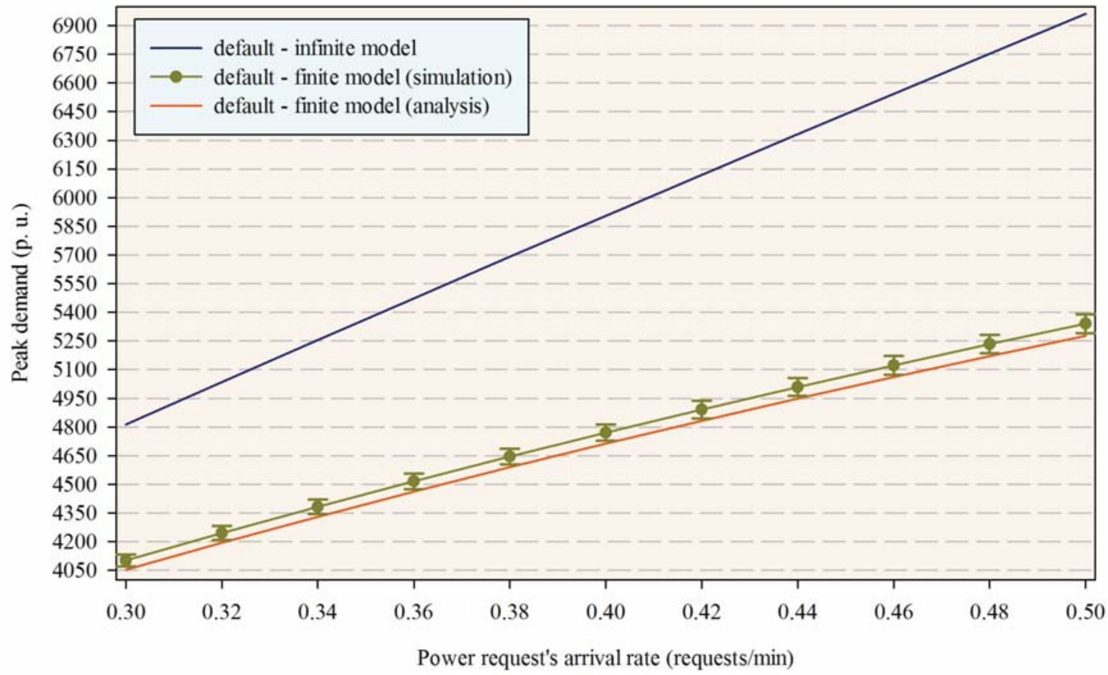

Figure C.5: Analytical results for the total number of requested p.u. under the default scenario for the infinite and the finite models.

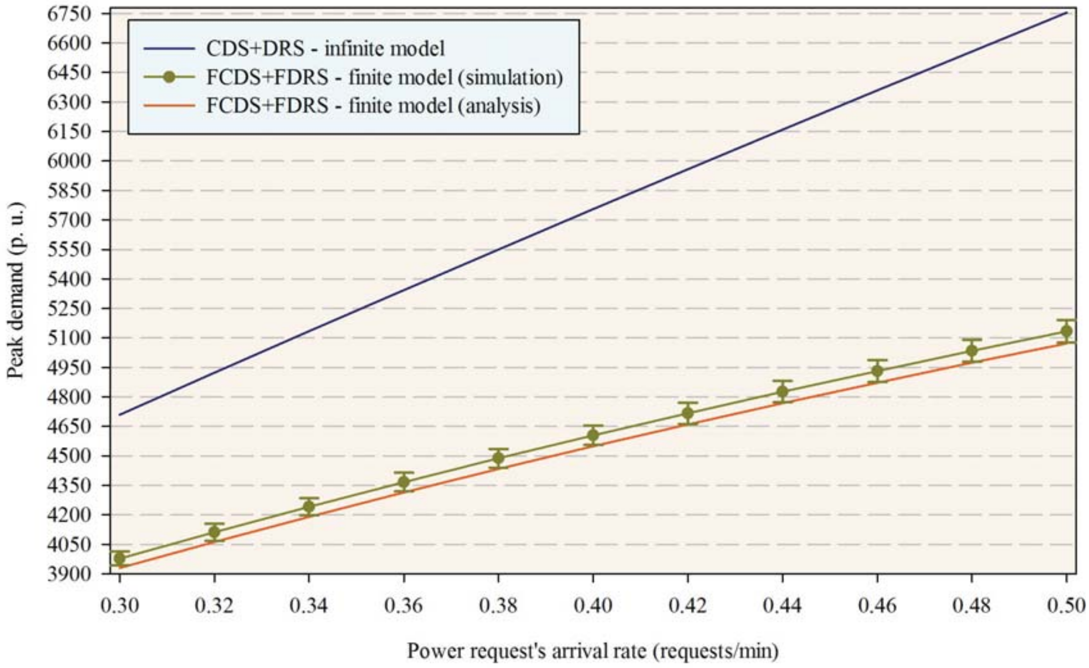

Figure C.6: Analytical results for the total number of requested p.u. under the combined FCDS+FDRS, for the infinite and the finite models.

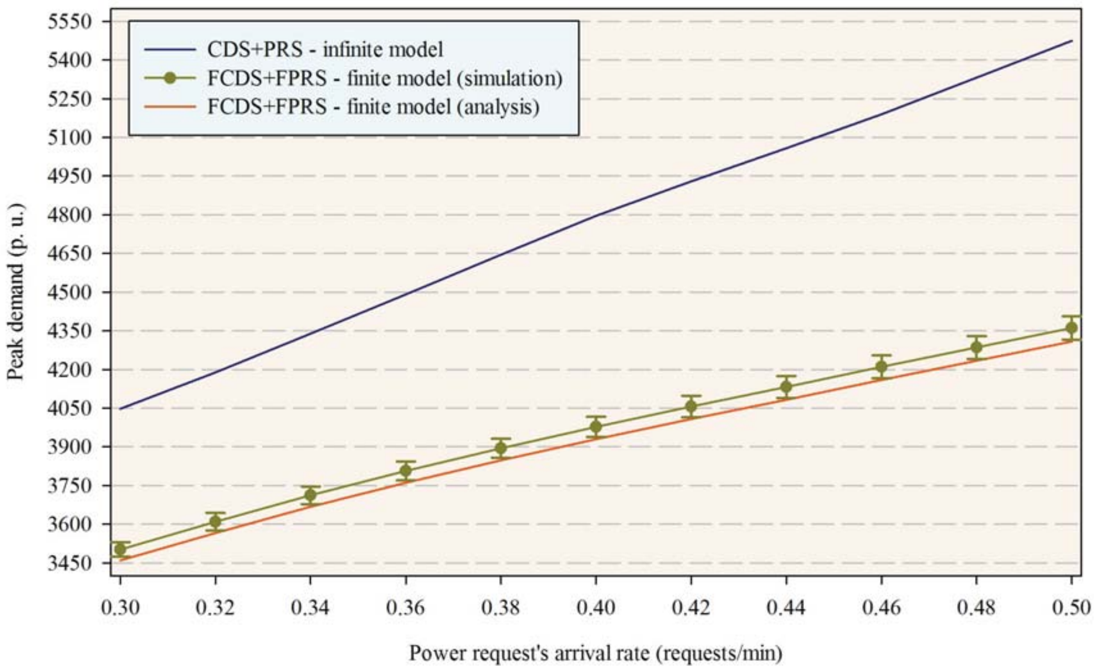

Figure C.7: Analytical results for the total number of requested p.u. under the combined FCDS+FPRS, for the infinite and the finite models.

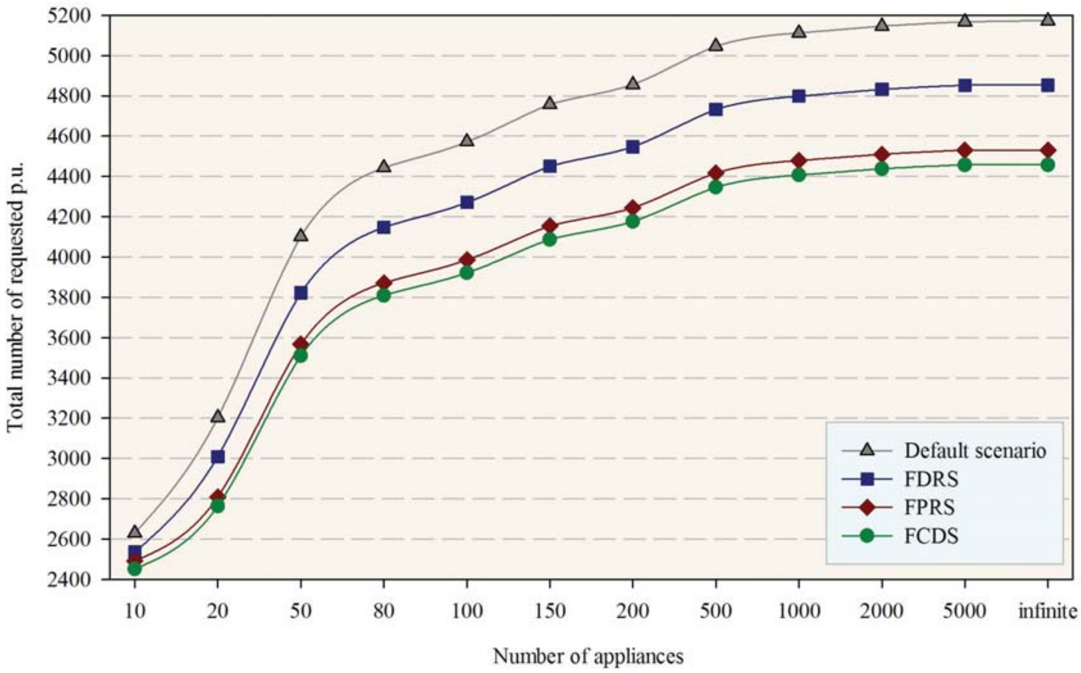

Figure C.8: Analytical results for the total number of requested p.u. versus the number of appliances, under the four scenarios.

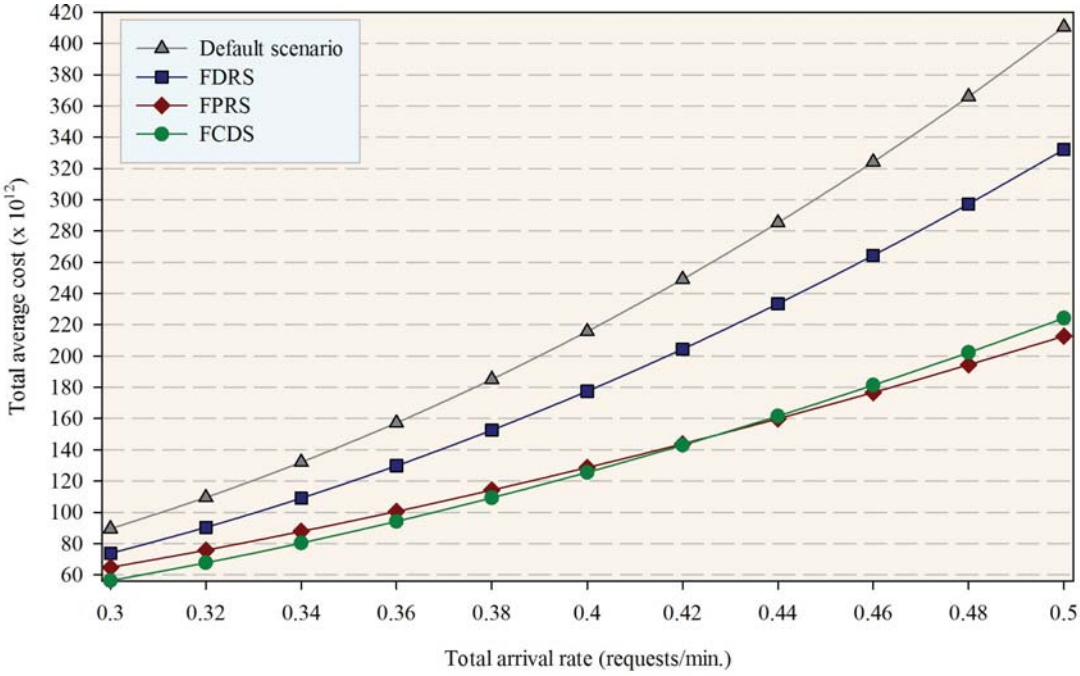

Figure C.9: Total average cost versus the total arrival rate, for the four different scenarios.

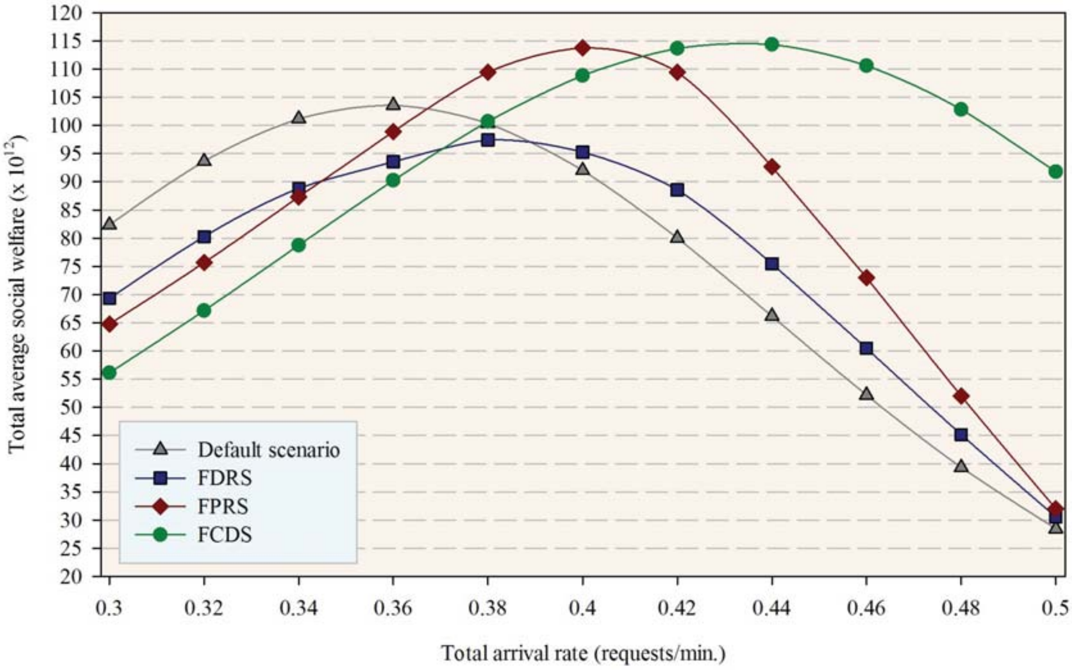

Figure C.10: Total average social welfare versus the total arrival rate, for the four different scenarios.

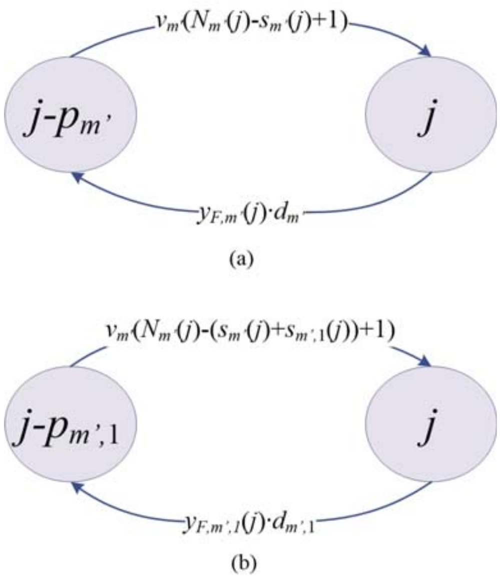

Figure C.11: State transition diagram of the system, under the FDRS when (a) $j – p_{m'} \leq P_0$, and, (b) $j - p_{m'} > P_0$.